

Supplemental information

Title: Muscle 4EBP1 activation modifies the structure and function of the neuromuscular junction in mice

Authors and affiliations:

Seok-Ting J. Ang^{1,2}, Elisa M. Crombie¹, Han Dong¹, Kuan-Ting Tan¹, Adriel Hernando¹, Dejie Yu^{2,3,4}, Stuart Adamson⁵, Seonyoung Kim¹, Dominic J. Withers^{6,7}, Hua Huang^{2,3,4} and Shih-Yin Tsai^{1,2}

¹Department of Physiology, Yong Loo Lin School of Medicine, National University of Singapore, Singapore, 117593, Singapore.

²Healthy Longevity Translational Research Programme, Yong Loo Lin School of Medicine, National University of Singapore, Singapore, 117456, Singapore

³Electrophysiology Core Facility, Yong Loo Lin School of Medicine, National University of Singapore, Singapore 117544, Singapore

⁴Cardiovascular Diseases Program, National University of Singapore, Singapore 117599, Singapore

⁵Buck Institute for Research on Aging, Novato, California, USA

⁶Metabolic Signalling Group, Medical Research Council Clinical Council London Institute of Medical Sciences (LMS), Du Cane Road, London W12 0NN, United Kingdom.

⁷Institute of Clinical Sciences (ICS), Faculty of Medicine, Imperial College London, Du Cane Road, London W12 0NN, United Kingdom.

This PDF file includes:

Supplementary Figure 1-7

Supplementary Table 1-7

Supplementary Figures

Supplementary Fig. 1: Molecular and histological analysis of the NMJ.

- a.** Quantification of the percentage of denervated NMJs in 6- and 28-month-old control male mice (using values from [Fig. 1d](#)). A denervated NMJ is defined as Mander's colocalization coefficient lower than 0.4. Sample size: 6mo Control, n=8 and 28mo Control, n=10; on average, 25 NMJs were analyzed per mouse. Statistical significance was determined by two-tailed unpaired student t-test.
- b.** qPCR of select AChR subunit and denervation-related genes in whole muscle lysate from 6- and 28- month-old control mice. Sample size: 6mo Control Female, n=3-5; 28mo Control Female, n=5-6; 6mo Control Male, n=3-4; 28mo Control Male, n=6-7. Statistical significance was determined by one-way ANOVA followed by Tukey's post-hoc pairwise comparison. Only a P value of less than 0.05 would be labeled in the figure.
- c.** Immunoblotting in quadriceps muscle of 12-month-old control and TSC1mKO mice. Ponceau red staining accompanying the immuoblots showing equal protein loading. Each lane represents individual mouse sample. Sample size: Control Male, n=4; TSC1mKO Male, n=4; Control Female, n=3; TSC1mKO Female, n=3.
- d.** Percentage distribution of AChR fragments of 12-month-old control (abbreviated as **C**), 12-month-old TSC1mKO (abbreviated as **T**), and 28-month-old control (abbreviated as **28C**) mice (analysis from [Fig. 3c](#)). Sample size: 12mo Control Female, n=3; 12mo TSC1mKO Female, n=4; 28mo Control Female, n=7; 12mo Control Male, n=4; 12mo TSC1mKO Male, n=3; 28mo Control Male, n=10; on average, 25 NMJs were analyzed per mouse. Statistical significance was determined by two-way ANOVA followed by Tukey multiple comparisons test. Only a P value of less than 0.05 would be labeled in the figure.
- e.** qPCR of select AChR subunit and denervation-related genes in whole muscle lysate from 12-month-old control and TSC1mKO mice. Sample size: 12mo Control Female, n=4-5; 12mo TSC1mKO Female, n=5-6; 12mo Control, n=5-7; TSC1mKO Male, n=5. Statistical significance was

determined by one-way ANOVA followed by Tukey's post-hoc pairwise comparison. Only a P value of less than 0.05 would be labeled in the figure.

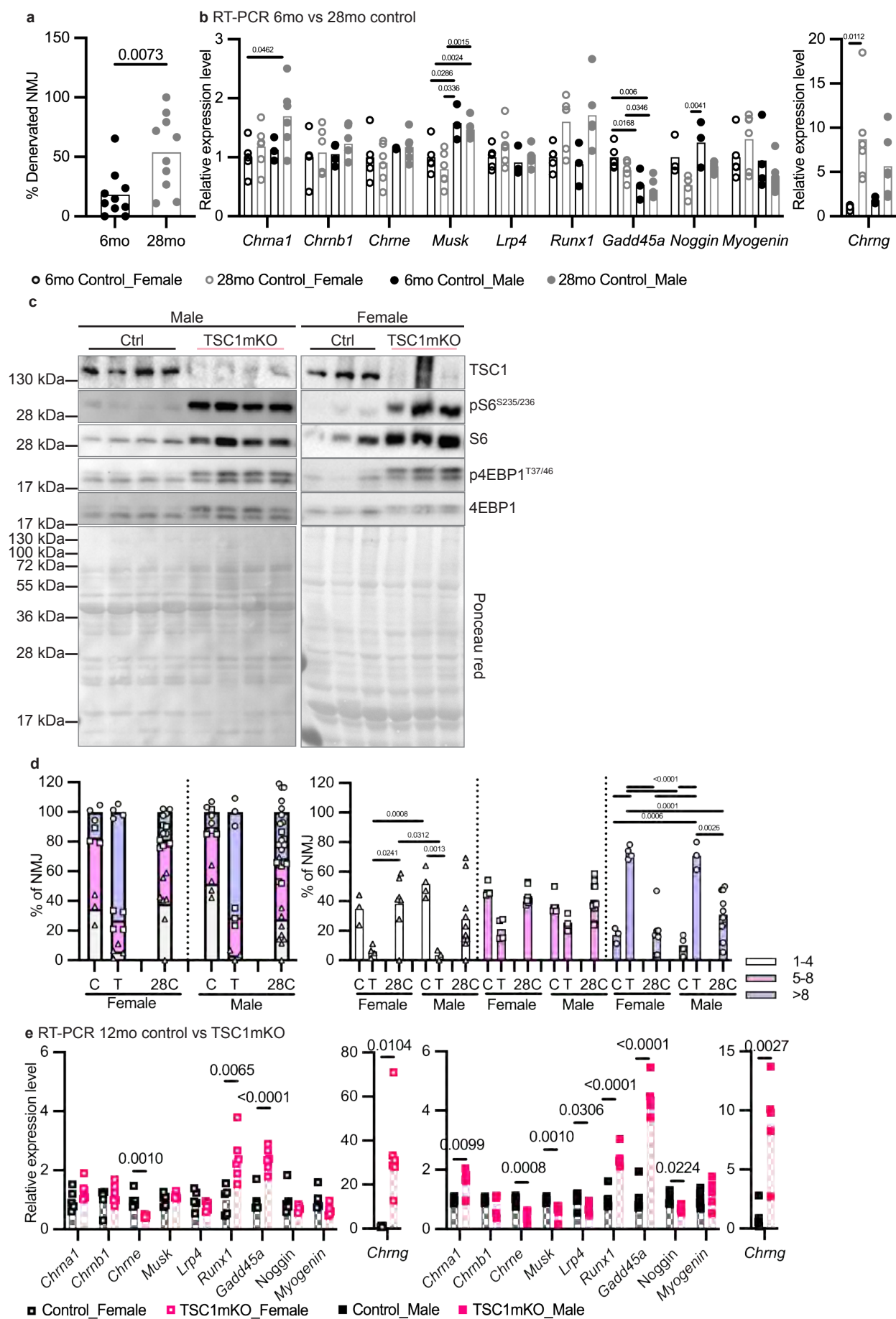


Figure S1

Supplementary Fig. 2: Myofiber analysis of S6K1mKO mice.

a-b. Representative H&E staining of (a) soleus and (b) tibialis anterior muscle from 6-month-old male mice (Control, n=4; S6K1mKO, n=3). Scale bars are indicated in the image.

c-d. Immunofluorescent staining for MyHC and WGA (white) (c) soleus (scale bar = 100 μ m) and (d) tibialis anterior (scale bar = 200 μ m) muscle from 6-month-old male mice (Control, n=4; S6K1mKO, n=3).

e-f. Quantification of cross-section size from selective MyHC in (e) soleus and (f) tibialis anterior muscle from male mice. Sample size: 6mo Control, n=3-4; 6mo S6K1mKO, n=3; 28mo Control, n=5; 28mo S6K1mKO, n=3-4; on average, ~6000-11000 myofibers were analyzed per mouse. Statistical significance: Data are shown as mean \pm SEM and statistical significance was determined by two-way ANOVA with Tukey's multiple comparison test compared within the size class. *P<0.05, **P<0.01, ***P<0.001, ****P<0.0001 indicates statistical significance of young versus old in either Control (black) or S6K1mKO (light blue) mice. #P<0.05, ##P<0.01, ###P<0.001, indicates significance of Control versus S6K1mKO in young (gray) mice.

g. Measurement of muscle coordination and strength by four limbs hanging test in 4-month-old male and female mice. Sample size: Control Male, n=20; S6K1mKO Male, n=26; Control Female, n=16; S6K1mKO Female, n=20. Statistical significance was determined by one-way ANOVA with Tukey's multiple comparison test compared within the same sex group. Only P<0.05 will be indicated in the graph.

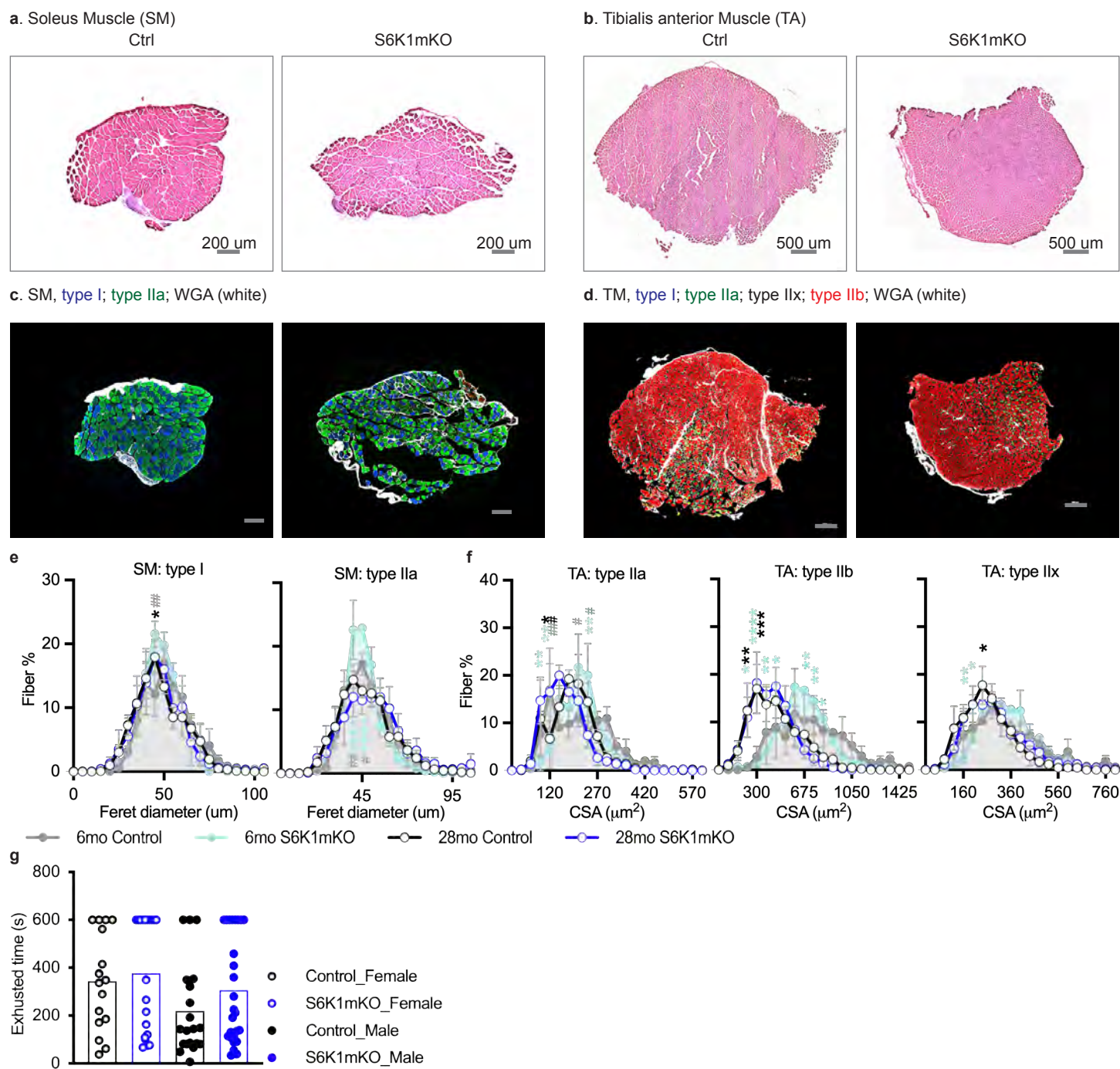


Figure S2

Supplementary Fig. 3: Muscle-specific deletion of *S6k1* attenuates intracellular pS6 accumulation during aging.

a. Representative confocal images of BTX (green), pS6^{S240+244} (red), DAPI (blue) and Laminin (white) staining from cross-sections of the gastrocnemius muscle of 6-month-old control (n=3) and S6K1mKO (n=3) male mice. The BTX and pS6^{S240+244} channels are shown in the bottom panels. Open arrow = junctional pS6^{S240+244}; Arrowhead = pS6^{S240+244} in the nucleus. Scale bar = 50μm.

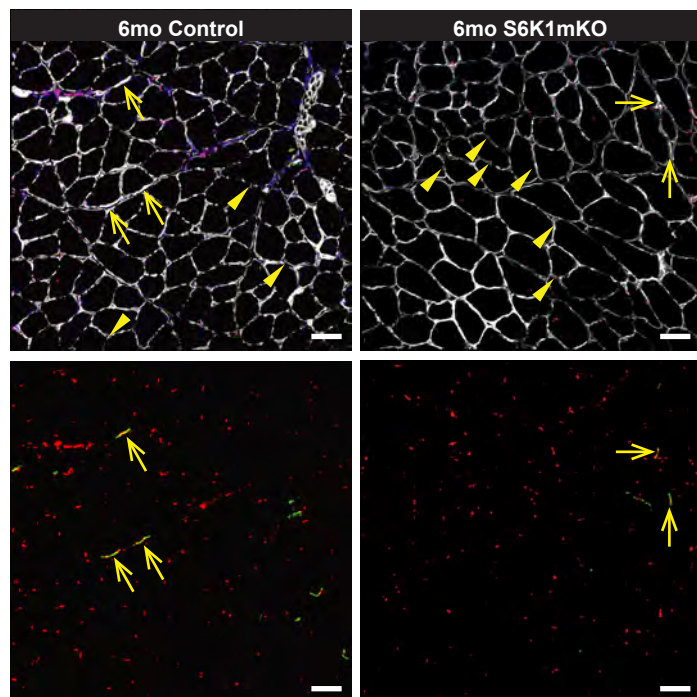
b. Representative confocal images of BTX (green), pS6^{S240+244} (red), DAPI (blue) and Laminin (white) staining from cross-sections of the gastrocnemius muscle of 12- and 28-month-old male mice (12mo S6K1-TSC1mKO, n=3; 28mo S6K1mKO, n=5). The insets are shown in the bottom panels. Asterisks = intracellular pS6^{S240+244} in angular, odd-shaped fibers; Arrowhead = pS6^{S240+244} in the nucleus, including central nucleus. Scale bars = 50μm.

c. Quantification of the percentage of pS6^{S240+244}-positive myofibers (left panel, one-way ANOVA followed by Tukey's post-hoc pairwise comparison) and mean CSA of pS6^{S240+244}-positive (pS6+) and pS6^{S240+244}-negative (pS6-) fibers (right panel, two-way ANOVA followed by Tukey's post-hoc pairwise comparison) in the gastrocnemius muscle sampled from 6-, 12-, and 28-month-old male mice. Sample size: 6mo Control and S6K1mKO Male, n=3 per group; 28mo Control Male, n=6; 28mo S6K1mKO Male, n=5; 12mo Control, TSC1mKO, and S6K1-TSC1mKO Male, n=3 per group; on average, 800 myofibers were analyzed per mouse. Detailed statistical analysis of CSA between groups within pS6- and pS6+ fibers is listed in [Supplementary Table. 1](#).

d. Immunoblotting of S6 phosphorylation at Ser240+244 and total S6 as well as total S6K1 in gastrocnemius muscle of 4-month-old control, S6K1mKO, TSC1mKO, and S6K1-TSC1mKO male mice. Ponceau red staining accompanying the immunoblots showing equal protein loading. Each lane represents individual mouse sample. Sample size: Control, n=11; S6K1mKO, n=4; TSC1mKO, n=4; TSC1-S6K1mKO, n=3; S6K1cko, n=1.

e. Immunoblotting of S6K2 phosphorylation at Ser423 and total S6K2 in gastrocnemius muscle of 4-month-old control and S6K1mKO male mice. Ponceau red staining accompanying the immunoblots showing equal protein loading. Each lane represents individual mouse sample. Sample size: Control, n=4; S6K1mKO, n=4; S6K1cko, n=1.

a BTX/pS6^{S240+244}/DAPI/Laminin (white)



b BTX/pS6^{S240+244}/DAPI/Laminin (white)

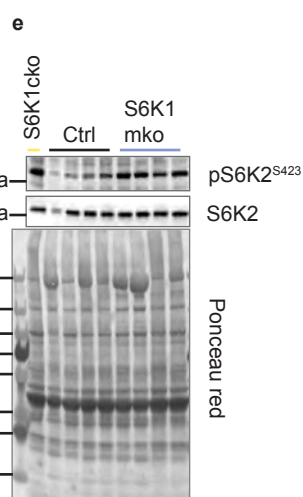
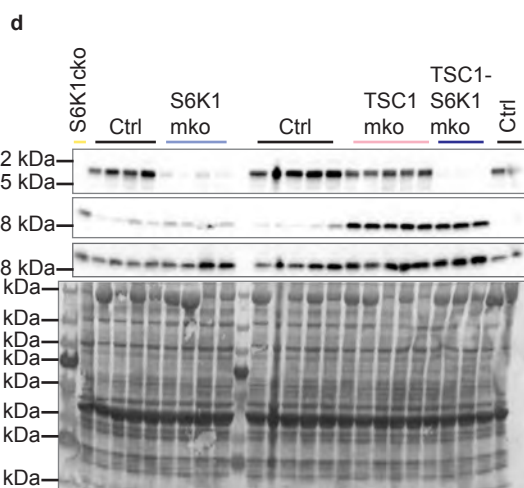
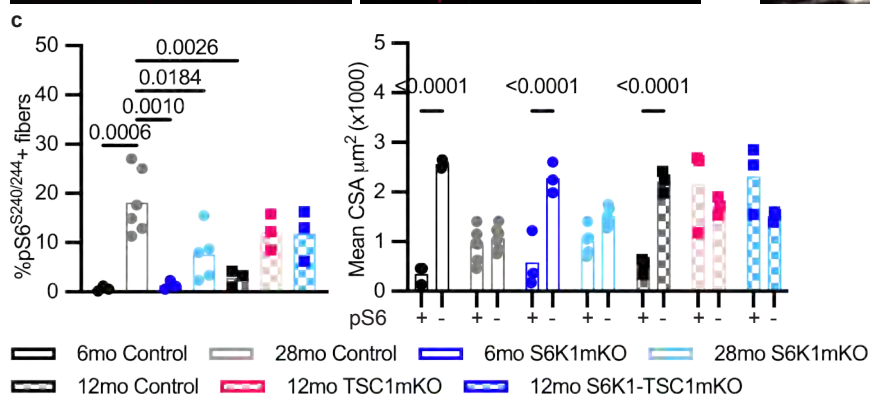
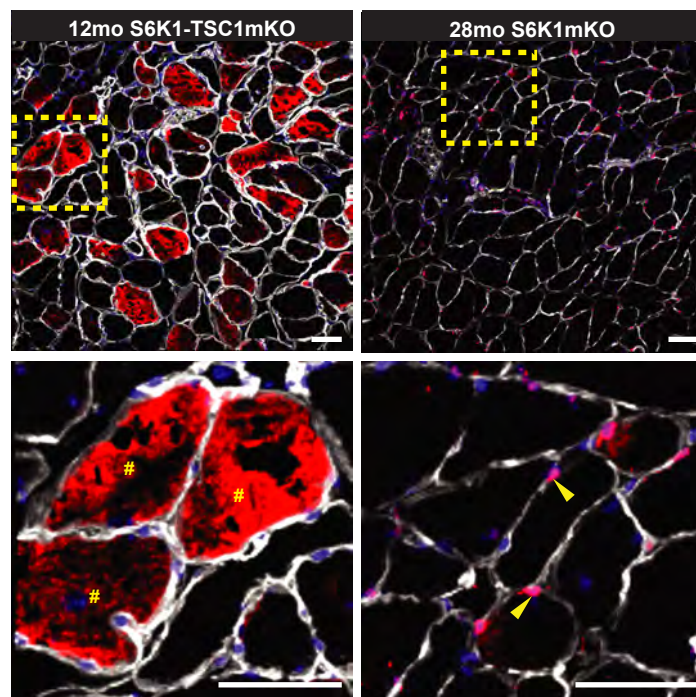


Figure S3

Supplementary Fig. 4: Muscle-specific deletion of *S6k1* has no effect on NMJ remodeling.

a. Representative confocal images of NMJs from longitudinal sections of the quadriceps muscle of male mice (28mo Control, n=10; 28mo S6K1mKO, n=4; 12mo Control, n=4; 12mo TSC1mKO and S6K1-TSC1mKO, n=3 per group). Top panels = BTX (green) and neurofilament (NF; red) + synaptophysin (Syn; red); Bottom panels = BTX (green) and DAPI (blue). Scale bar = 20µm.

b-e. Quantification of NMJ morphological properties which include **(b)** the number of AChR fragmentation, **(c)** the number of post-synaptic myonuclei, **(d)** Mander's colocalization coefficient, and **(e)** quantification of the percentages of NCAM-positive myofibers.

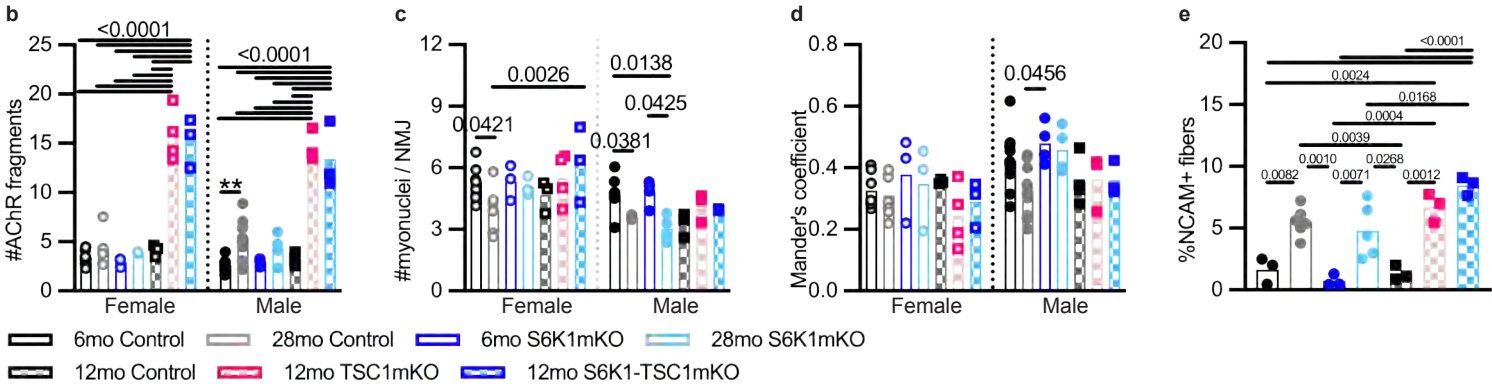
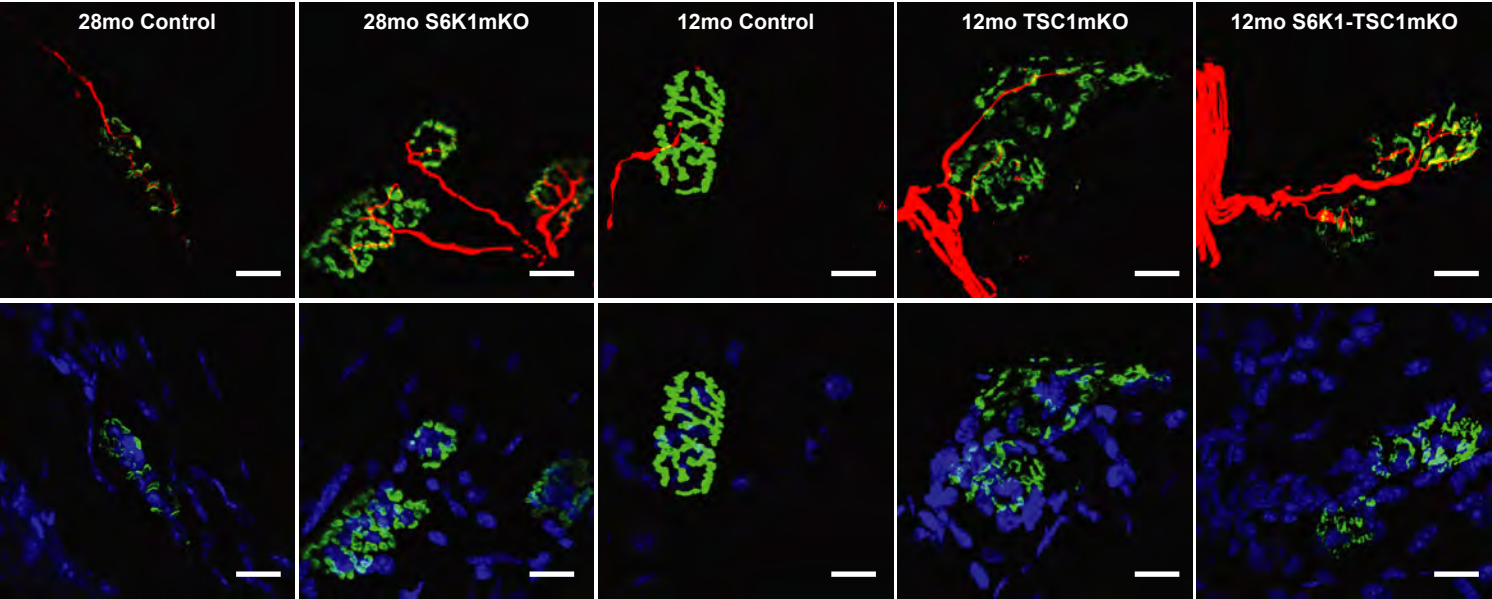
f. Representative confocal images of BTX (green), NCAM (red), DAPI (blue) and Laminin (white) staining from cross-sections of the gastrocnemius muscle of male mice (6mo Control, n=3; 28mo Control, n=6; 28mo S6K1mKO, n=5; 12mo Control, TSC1mKO, and S6K1-TSC1mKO Male, n=3 per group). Scale bars = 50µm.

Sample size: NMJ quantification ([Supplementary Fig. 4b-d](#)), 6mo and 28mo Control Female, n=7 per group; 6mo and 28mo S6K1mKO Female, n=3 per group; 12mo Control and S6K1-TSC1mKO Female, n=3 per group; 12mo TSC1mKO Female, n=4; 6mo and 28mo Control Male, n=10 per group; 6mo and 28mo S6K1mKO Male, n=4 per group; 12mo Control Male, n=4; 12mo TSC1mKO and S6K1-TSC1mKO Male, n=3 per group; on average, 25 NMJs were analyzed per animal.

Myofiber analysis of NCAM ([Supplementary Fig. 4e](#)), 6mo Control and S6K1mKO Male, n=3 per group; 28mo Control Male, n=6; 28mo S6K1mKO Male, n=5; 12mo Control, TSC1mKO, and S6K1-TSC1mKO Male, n=3 per group; on average, 800 myofibers were analyzed per mouse.

Statistical significance: NMJ quantification ([Supplementary Fig. 4b-d](#)), two-way ANOVA followed by Tukey's post-hoc pairwise comparison; Myofiber analysis of NCAM ([Supplementary Fig. 4e](#)), one-way ANOVA followed by Tukey's post-hoc pairwise comparison. Only P<0.05 will be indicated in the graph.

a BTX / NF + Syn / DAPI



f BTX / NCAM / DAPI / Laminin (white)

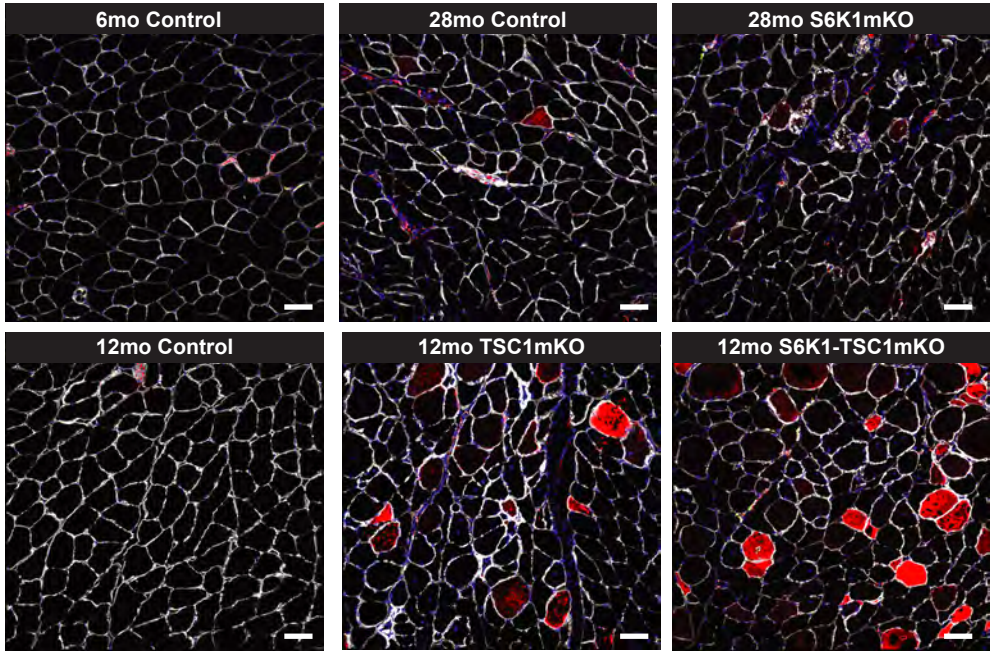


Figure S4

Supplementary Fig. 5: Molecular and histological analysis of NMJ with activation of 4EBP1 in the skeletal muscle.

a-b. Quantification of (a) endplate area and (b) AChR area of 6-month-old male control (n=5) and 4EBP1mt-muscle (n=3).

c-d. Percentage distribution of (c) number of fragments from further analysis of Fig. 4d, and (d) number of post-synaptic myonuclei from further analysis of Fig. 4e of 6-month-old and 28-month-old male control and 4EBP1mt-muscle, as well as 12-month-old male control (abbreviated as **C**), TSC1mKO (abbreviated as **T**) and 4EBP1mt-TSC1mKO (abbreviated as **ET**). Sample size: 6mo and 28mo Control, n=10 per group; 6mo 4EBP1mt-muscle, n=4; 28mo 4EBP1mt-muscle, n=5; 12mo Control and 4EBP1mt-TSC1mKO, n=4 per group; 12mo TSC1mKO, n=3 per group; on average, 25 NMJs were analyzed per animal.

e-g. qPCR of select AChR subunit genes and denervation-related genes in whole muscle lysate from (e) 6-month-old male control (n=4) and 4EBP1mt-muscle (n=3); (f) 12-month-old female control (n=4-5), TSC1mKO (n=5-6), S6K1-TSC1mKO (n=6-7), and 4EBP1mt-TSC1mKO (n=4); (g) 12-month-old male control (n=5-7), TSC1mKO (n=5), S6K1-TSC1mKO (n=4), and 4EBP1mt-TSC1mKO (n=4).

h. Immunoblotting in gastrocnemius muscle of 12-month-old female control, TSC1mKO, 4EBP1mt-TSC1mKO, and S6K1-TSC1mKO (n=3 per group). Ponceau red staining accompanying the immunoblots showing equal protein loading. Each lane represents individual mouse sample.

Statistical significance: Two-tailed unpaired student t-test for Supplementary Fig. 5a, 5b, and 5e. One-way ANOVA followed by Tukey post-hoc pairwise comparison for Supplementary Fig. 5f and 5g. Only $P < 0.05$ will be indicated in the graph.

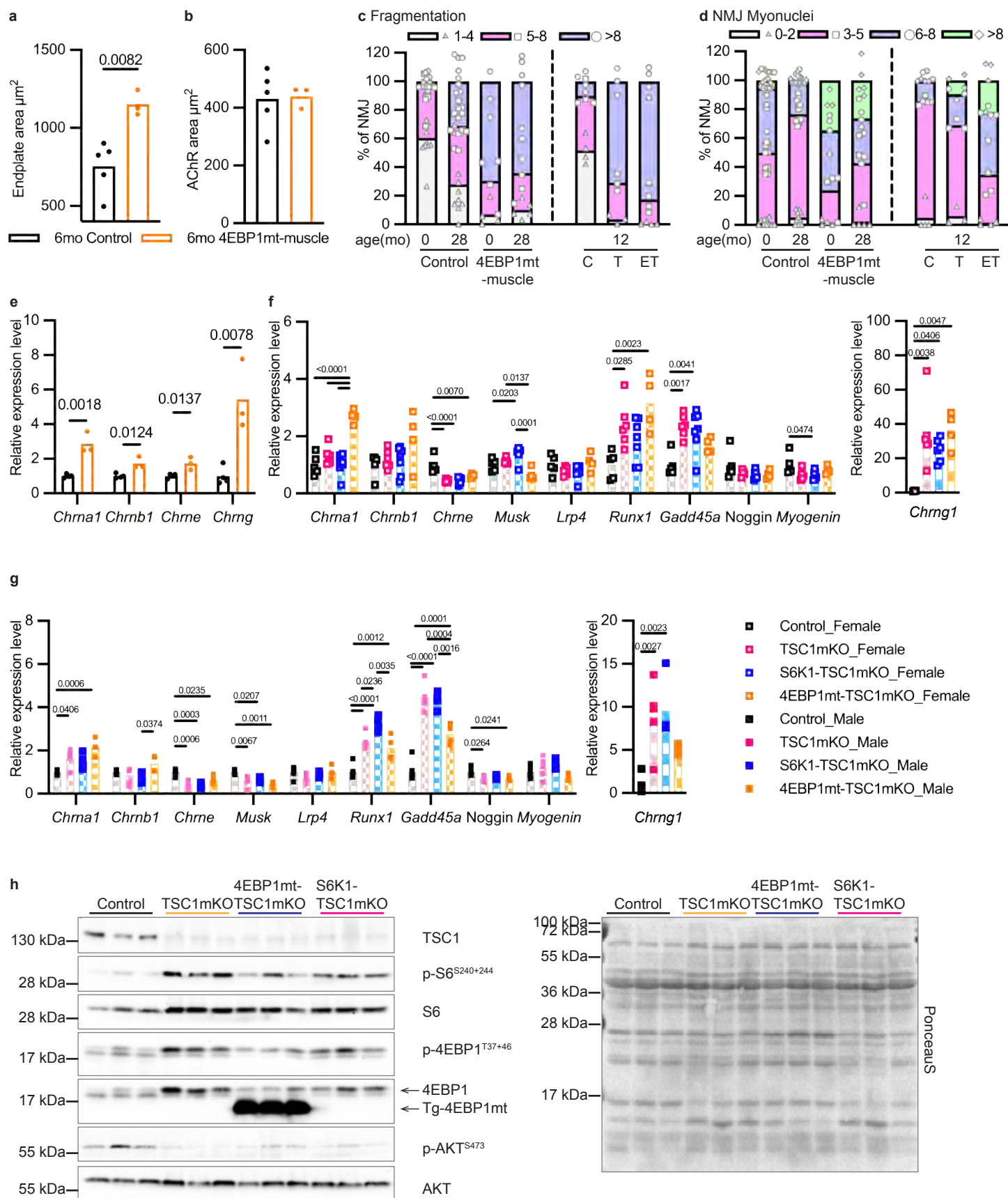


Figure S5

Supplementary Fig. 6: Pathology analysis of TSC1mKO mouse myofiber.

a-b. Representative H&E staining of **(a)** tibialis anterior and **(b)** soleus muscle from 12-month-old male mice (n=4 per group). Black arrows, myofibers with inclusions; white arrows, degenerated basophilic fibers. Scale bar, 50 μ m.

c. Measurement of muscle coordination and strength by four limbs hanging test in 4-month-old male and female mice. Sample size: Control Male, n=24; TSC1mKO Male, n=12; TSC1-S6K1mKO Male, n=17; 4EBP1mt-TSC1mKO Male, n=9; Control Female, n=31; TSC1mKO Female, n=16; TSC1-S6K1mKO Female, n=27; 4EBP1mt-TSC1mKO Female, n=6. Statistical significance was determined by one-way ANOVA with Tukey's multiple comparison test of the same sex group. Only $P < 0.05$ will be indicated in the graph.

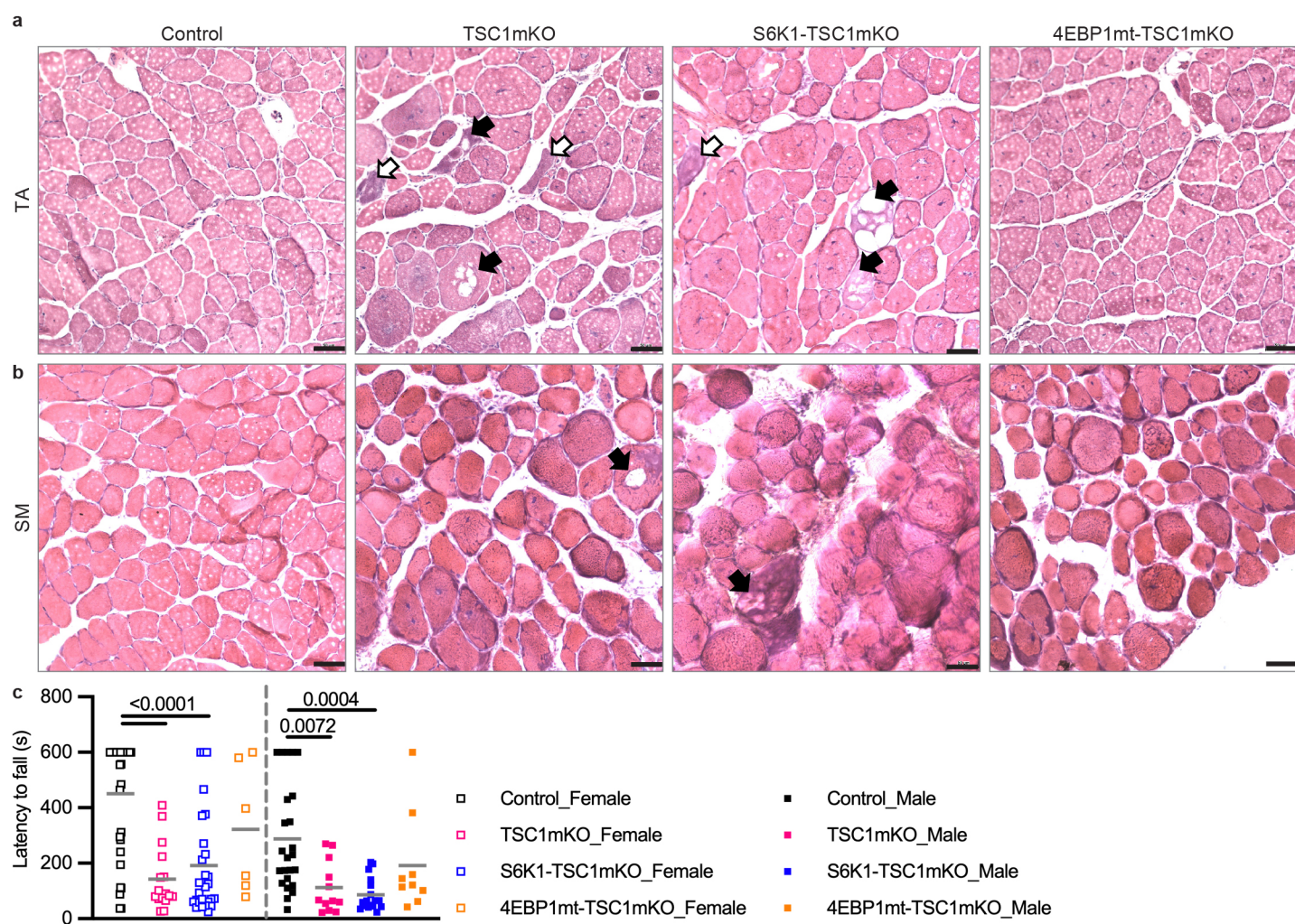


Figure S6

Supplementary Fig. 7: Activation of 4EBP1 in the skeletal muscle enhances NMJ synaptic transmission and myofiber regeneration.

a. Representative confocal images of NMJs from longitudinal sections of the quadriceps muscle from 3-month-old male mice (Control, n=4; 4EBPmt-muscle, n=3). BTX (green) and neurofilament (NF; red) + synaptophysin (Syn; red); Scale bar = 20 μ m.

b. Representative traces of miniature endplate potential (mEPP, top) and EPP (bottom) recorded from the diaphragm of 3-month-old male mice (n=6 per group).

c. Normalized EPP (to first pulse) recorded in the diaphragm in response to repeated phrenic nerve stimulation at 10Hz (n=6 per group).

d-e. Percentages of central nucleated fibers sampled from the gastrocnemius muscle of **(d)** 28-month-old control (n=6) and 4EBP1mt-muscle (n=3) male mice, as well as **(e)** 12-month-old control, TSC1mKO, 4EBP1mt-TSC1mKO male mice (n=3 per group). Data are presented as mean values \pm SEM. Statistical significance was determined by two-tailed unpaired student t-test for [Supplementary Fig. 7d](#) and one-way ANOVA followed by Tukey post-hoc pairwise comparison for [Supplementary Fig. 7e](#). Only P<0.05 will be indicated in the graph.

a BTX / NF + Syn

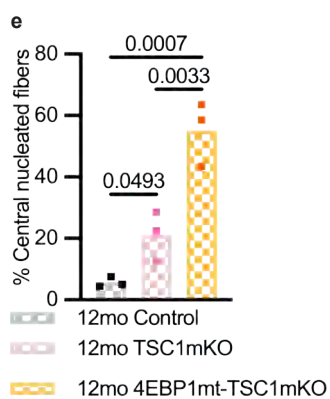
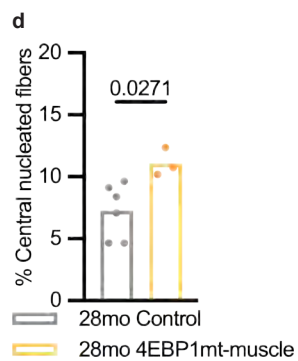
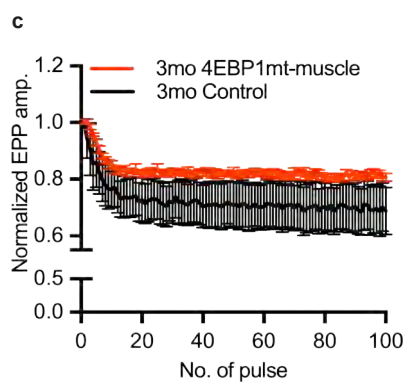
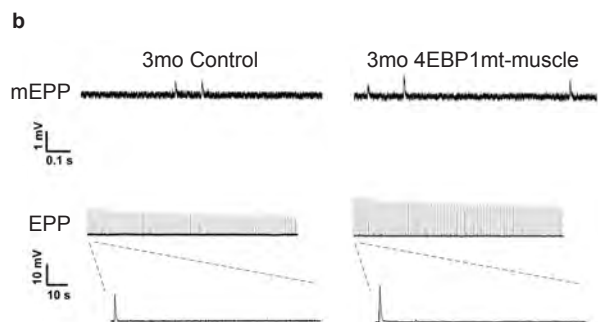
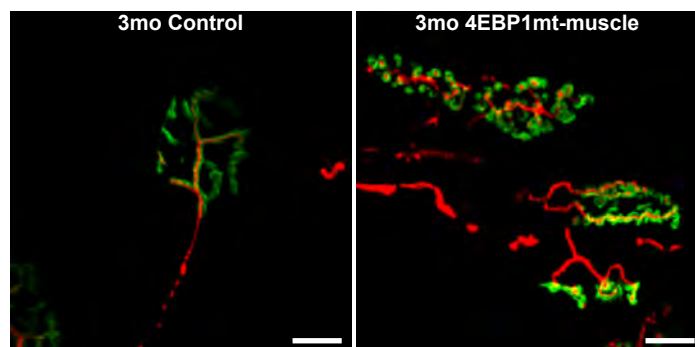


Figure S7

Supplementary Table 1Statistical analysis of CSA quantification between groups ([Supplementary Fig. 3C](#)).

two-way ANOVA pS6+	6mo Contro l	28mo Contro l	6mo S6K1mK O	28mo S6K1mK O	12mo Contro l	12mo TSC1mK O	12mo S6K1- TSC1mK O
6mo Control						<0.0001	<0.0001
28mo Control						0.004	<0.0001
6mo S6K1mK O						<0.0001	<0.0001
28mo S6K1mK O						0.014	0.003
12mo Control						<0.0001	<0.0001
12mo TSC1mK O	<0.0001	0.004	<0.0001	0.014	<0.0001		
12mo S6K1- TSC1mK O	<0.0001	<0.0001	<0.0001	0.003	<0.0001		
two-way ANOVA pS6-	6mo Contro l	28mo Contro l	6mo S6K1mK O	28mo S6K1mK O	12mo Contro l	12mo TSC1mK O	12mo S6K1- TSC1mK O
6mo Control		<0.0001		0.0046			0.0148
28mo Control	<0.0001		0.0005		0.0012		
6mo S6K1mK O				0.0005			
28mo S6K1mK O	0.0046						
12mo Control		0.0012					
12mo TSC1mK O							
12mo S6K1- TSC1mK O	0.0148						

Supplementary Table 2. List of PCR primers used in this study

	Forward	Reverse
<i>Chrna1</i>	TGGACCTATGACGGCTCTGT	GGAGTAGAACACCCAGTGCT
<i>Chrnbl</i>	ACGTTGCCCTGGACATCAAT	CAACCGAGAGGTTTGGGTCA
<i>Chrne</i>	CGCTATGAGGGAGGTTCCAC	GACAGTCTGGGCTAGCAGGA
<i>Chrng</i>	AGGCAGCGCAATGGATTAGT	TTACAGGCATCCACACAGGC
<i>Musk</i>	ACTGCGTGGAATGAGCTGAA	TCCATTGCCTGCCATTCCTT
<i>Lrp4</i>	GTGTGTGACGGGGACAATG	GCATTGCTCGTCACTGTTGT
<i>NCAM</i>	TGACGACTCCTCTACCCTCAC	AATCACAGCATCCTCCCCTTC
<i>Runx1</i>	GCCATGAAGAACCAGGTAGC	GCCGTCCACTGTGATTTTG
<i>Gadd45a</i>	GAAAGTCGCTACATGGATCAGT	AAACTTCAGTGCAATTTGGTTC
<i>Noggin</i>	TCTTGGCTACAGAGACCTGG	GAAGCCGGGTAAC TTTTGACG
<i>Myogenin</i>	CTACAGGCCTTGCTCAGCTC	TGGGACCGAACTCCAGTG

Supplementary Table 3. List of RNAScope probes

Gene	Species	Channel	Catalogue no.
<i>Chrne</i>	Mouse	C3	832701
<i>Eif4ebp1</i>	Mouse	C1	439321

Supplementary Table 4

Statistical analysis of the number of AChR fragmentation (Fig. 4d).

two-way ANOVA female	6mo Control	28mo Control	6mo 4EBP1mt-muscle	28mo 4EBP1mt-muscle	12mo Control	12mo TSC1mKO	12mo 4EBP1mt-TSC1mKO
6mo Control		0.9997	0.1093	0.0086 **	>0.9999	<0.0001 ****	<0.0001 ****
28mo Control	0.9997		0.2227	0.0230 *	>0.9999	0.0001 ***	<0.0001 ****
6mo 4EBP1mt-muscle	0.1093	0.2227		0.9783	0.4399	0.2814	<0.0001 ****
28mo 4EBP1mt-muscle	0.0086 **	0.0230 *	0.9783		0.1009	0.7947	<0.0001 ****
12mo Control	>0.9999	>0.9999	0.4399	0.1009		0.0026 **	<0.0001 ****
12mo TSC1mKO	<0.0001 ****	0.0001 ***	0.2814	0.7947	0.0026 **		<0.0001 ****
12mo 4EBP1mt-TSC1mKO	<0.0001 ****	<0.0001 ****	<0.0001 ****	<0.0001 ****	<0.0001 ****	<0.0001 ****	
two-way ANOVA Male	6mo Control	28mo Control	6mo 4EBP1mt-muscle	28mo 4EBP1mt-muscle	12mo Control	12mo TSC1mKO	12mo 4EBP1mt-TSC1mKO
6mo Control		0.6134	0.0100 *	<0.0001 ****	>0.9999	0.0001 ***	<0.0001 ****
28mo Control	0.6134		0.2413	0.0099 **	0.9518	0.0069 **	<0.0001 ****
6mo 4EBP1mt-muscle	0.0100 *	0.2413		0.9704	0.0932	0.7867	0.0005 ***
28mo 4EBP1mt-muscle	<0.0001 ****	0.0099 **	0.9704		0.0052 **	0.9943	0.0047 **
12mo Control	>0.9999	0.9518	0.0932	0.0052 **		0.0031 **	<0.0001
12mo TSC1mKO	0.0001 ***	0.0069 **	0.7867	0.9943	0.0031 **		0.0967
12mo 4EBP1mt-TSC1mKO	<0.0001 ****	<0.0001 ****	0.0005 ***	0.0047 **	<0.0001	0.0967	

Supplementary Table 5

Statistical analysis of the number of post-synaptic myonuclei (Fig. 4e).

two-way ANOVA female	6mo Control	28mo Control	6mo 4EBP1mt-muscle	28mo 4EBP1mt-muscle	12mo Control	12mo TSC1mKO	12mo 4EBP1mt-TSC1mKO
6mo Control		0.5211	0.0175 *	0.0199 *	0.9933	>0.9999	0.0018 **
28mo Control	0.5211		0.0001 ***	0.0001 ***	0.9883	0.5556	<0.0001 ****
6mo 4EBP1mt-muscle	0.0175 *	0.0001 ***		>0.9999	0.0177 *	0.0812	0.9608
28mo 4EBP1mt-muscle	0.0199 *	0.0001 ***	>0.9999		0.0197 *	0.0893	0.9530
12mo Control	0.9933	0.9883	0.0177 *	0.0197 *		0.9847	0.0023 **
12mo TSC1mKO	>0.9999	0.5556	0.0812	0.0893	0.9847		0.0110 *
12mo 4EBP1mt-TSC1mKO	0.0018 **	<0.0001 ****	0.9608	0.9530	0.0023 **	0.0110 *	
two-way ANOVA Male	6mo Control	28mo Control	6mo 4EBP1mt-muscle	28mo 4EBP1mt-muscle	12mo Control	12mo TSC1mKO	12mo 4EBP1mt-TSC1mKO
6mo Control		0.5062	<0.0001 ****	0.0019 **	0.6007	0.9956	0.1568
28mo Control	0.5062		<0.0001 ****	<0.0001 ****	>0.9999	0.9949	0.0035 **
6mo 4EBP1mt-muscle	<0.0001 ****	<0.0001 ****		0.9041	<0.0001 ****	0.0005 ***	0.3173
28mo 4EBP1mt-muscle	0.0019 **	<0.0001 ****	0.9041		0.0001 ***	0.0085 **	0.9122
12mo Control	0.6007	>0.9999	<0.0001 ****	0.0001 ***		0.9843	0.0115 *
12mo TSC1mKO	0.9956	0.9949	0.0005 ***	0.0085 **	0.9843		0.1692
12mo 4EBP1mt-TSC1mKO	0.1568	0.0035 **	0.3173	0.9122	0.0115 *	0.1692	

Supplementary Table 6

Statistical analysis of Mander's colocalization coefficient (Fig. 4f).

two-way ANOVA female	6mo Control	28mo Control	6mo 4EBP1mt-muscle	28mo 4EBP1mt-muscle	12mo Control	12mo TSC1mKO	12mo 4EBP1mt-TSC1mKO
6mo Control		>0.9999	0.9997	0.8082	0.9875	0.8087	0.0319 *
28mo Control	>0.9999		0.9995	0.7869	0.9890	0.7865	0.0288 *
6mo 4EBP1mt-muscle	0.9997	0.9995		0.9691	0.9401	0.9690	0.1257
28mo 4EBP1mt-muscle	0.8082	0.7869	0.9691		0.4934	>0.9999	0.5382
12mo Control	0.9875	0.9890	0.9401	0.4934		0.4929	0.0162 **
12mo TSC1mKO	0.8087	0.7865	0.9690	>0.9999	0.4929		0.5386
12mo 4EBP1mt-TSC1mKO	0.0319 *	0.0288 *	0.1257	0.5382	0.0162 **	0.5386	
two-way ANOVA Male	6mo Control	28mo Control	6mo 4EBP1mt-muscle	28mo 4EBP1mt-muscle	12mo Control	12mo TSC1mKO	12mo 4EBP1mt-TSC1mKO
6mo Control		0.0754	0.0031 **	0.0081 **	0.7258	0.8797	0.0760
28mo Control	0.0754		0.5285	0.8247	0.9944	0.9897	0.9919
6mo 4EBP1mt-muscle	0.0031 **	0.5285		0.9985	0.3744	0.3915	0.9622
28mo 4EBP1mt-muscle	0.0081 **	0.8247	0.9985		0.6310	0.6347	0.9990
12mo Control	0.7258	0.9944	0.3744	0.6310		>0.9999	0.9140
12mo TSC1mKO	0.8797	0.9897	0.3915	0.6347	>0.9999		0.8996
12mo 4EBP1mt-TSC1mKO	0.0760	0.9919	0.9622	0.9990	0.9140	0.8996	

Supplementary Table 7Statistical analysis of quantification of the percentages of NCAM-positive myofibers ([Fig. 4g](#)).

one-way ANOVA	3mo Control	28mo Control	3mo 4EBP1mt-muscle	28mo 4EBP1mt-muscle	12mo Control	12mo TSC1mKO	12mo 4EBP1mt-TSC1mKO
3mo Control		<0.0001 #####	0.0509	0.0004 ###	0.9807	<0.0001 #####	0.0160 #
28mo Control	<0.0001 #####		0.0572	>0.9999	0.0006 ###	0.7120	0.4065
3mo 4EBP1mt-muscle	0.0509	0.0572		0.1877	0.3303	0.0081 ##	0.9820
28mo 4EBP1mt-muscle	0.0004 ###	>0.9999	0.1877		0.0039 ##	0.7549	0.6470
12mo Control	0.9807	0.0006 ###	0.3303	0.0039 ##		0.0002 ###	0.1209
12mo TSC1mKO	<0.0001 #####	0.7120	0.0081 ##	0.7549	0.0002 ###		0.0669
12mo 4EBP1mt-TSC1mKO	0.0160 #	0.4065	0.9820	0.6470	0.1209	0.0669	